International Journal of Nanomedicine

Dovepress
open access to scientific and medical research

Open Access Full Text Article

ORIGINAL RESEARCH

Enhanced Dissolution and Bioavailability of Curcumin Nanocrystals Prepared by Hot Melt Extrusion Technology

Yujie Zhao[1], Xiaoyin Xu[1], Anyin Dai[2], Yunxiang Jia[1], Wenxi Wang[1]

[1]College of Pharmacy, Zhejiang University of Technology, Hangzhou, People's Republic of China; [2]Department of Pharmacy, The 903rd Hospital of People's Liberation Army, Hangzhou, People's Republic of China

Correspondence: Wenxi Wang, College of Pharmacy, Zhejiang University of Technology, 18# Chaowang Road, Hangzhou, Zhejiang, 310014, People's Republic of China, Tel +86 571 8832 0772, Fax +86 571 8832 0320, Email yjw@zjut.edu.cn

Purpose: Curcumin nanocrystals (Cur-NCs) were prepared by hot melt extrusion (HME) technology to improve the dissolution and bioavailability of curcumin (Cur).

Methods: Cur-NCs with different drug-carrier ratios were prepared by one-step extrusion process with Eudragit® EPO (EEP) as the carrier. The dispersed size and solid state of Cur in extruded samples were characterized by dynamic light scattering (DLS), scanning electron microscope (SEM), differential scanning calorimetry (DSC), and X-ray diffraction (XRD). The thermal stability of Cur was analyzed by thermogravimetric analysis (TGA) and high performance liquid chromatography (HPLC). Dissolution and pharmacokinetics were studied to evaluate the improvement of dissolution and absorption of Cur by nano-preparation.

Results: Cur-NCs with particle sizes in the range of 50~150 nm were successfully prepared by using drug-carrier ratios of 1:1, 2:1 and 4:1, and the crystal form of Cur was Form 1 both before and after HME. The extrudate powders showed very efficient dissolution with the cumulative dissolution percentage of 80% in less than 2 min, and the intrinsic dissolution rates of them were 13.68 ± 1.20 mg/min/cm^2, 11.78 ± 0.57 mg/min/cm^2 and 4.35 ± 0.20 mg/min/cm^2, respectively, whereas that of pure Cur was only 0.04 ± 0.00 mg/min/cm^2. The TGA data demonstrated that the degradation temperature of Cur was about 250 °C, while the HPLC results showed Cur was degraded when extruded at the temperature over 150 °C. Pharmacokinetic experiment showed a significant improvement in the absorption of Cur. The C_{max} of Cur in the Cur-NC group was 1.68 times that of pure Cur group, and the C_{max} and area under the curve ($AUC_{0-\infty}$) of metabolites were 2.79 and 4.07 times compared with pure Cur group.

Conclusion: Cur-NCs can be prepared by HME technology in one step, which significantly improves the dissolution and bioavailability of Cur. Such a novel method for preparing insoluble drug nanocrystals has broad application prospects.

Keywords: hot melt extrusion technology, curcumin, nanocrystals, dissolution, absorption in vivo

Introduction

As a natural antioxidant,[1] Curcumin (Cur) is a polyphenolic compound extracted from the rhizome of Curcuma longa and is frequently used as a food-flavoring agent, colorant, and traditional medicine.[2–4] Due to its extensive antimicrobial, anti-inflammatory, antioxidant, neuroprotective, and immunomodulatory properties,[3,5] Cur has exhibited excellent therapeutic benefits in various diseases, such as cancer (including gastrointestinal, hematological, gynecological, and urinary cancer),[6] cardiovascular disease, Alzheimer's disease, inflammatory disease, nervous system disease and so on.[7–10] Unfortunately, despite Cur's wide range of potential applications, its practical use is limited by its poor solubility and permeability, high metabolic activity, and low bioavailability.[5,11,12] To increase the solubility and bioavailability of Cur, prevent its degradation and metabolism, and enhance its ability to target cancer, significant advancements have been made in the development of polymer nanoparticles, polymer micelles, liposomes, nanogels, solid lipid nanoparticles, polymer conjugates, self-assembly nano drug delivery systems and other nano-preparations.[1,5,7,13–16]

Received: 16 February 2024
Accepted: 29 May 2024
Published: 12 June 2024

Graphical Abstract

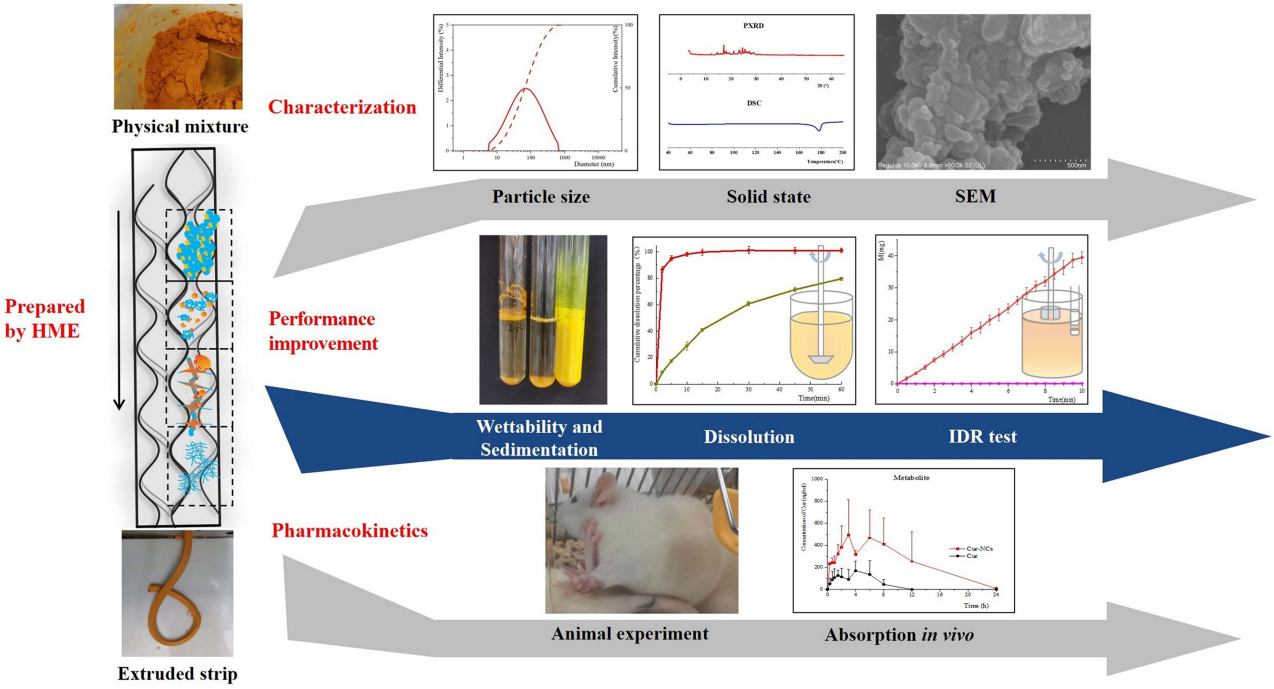

With their high drug loading, good stability, low toxicity and side effects, and simple preparation,[17] nanocrystals (NCs) have emerged as one of the most promising approaches to improve the pharmaceutical performance of hydrophobic drugs. Not only are they suitable for oral administration, but also they can be administered via parenteral, transdermal, ocular, pulmonary, and intranasal routes.[18–21] There are two types of techniques known for the preparation of nanocrystals: top-down and bottom-up.[21–23] The former primarily employs methods including wet grinding and high-pressure homogenization. For example, Rossetti et al[24] prepared atorvastatin calcium nanocrystal suspension by wet grinding, and Bhaskar et al[25] obtained cefixime trihydrate nanocrystal suspension though high-pressure homogenization technology. Both preparation methods have been applied to industrial manufacturing.[19,23,26] The latter mainly uses techniques such as anti-solvent precipitation, supercritical fluid, or spray freeze drying to control the nucleation and crystal growth processes so as to prepare nanocrystals.[23,27] Chen et al[28] prepared protopanaxadiol nanocrystals suspension by anti-solvent precipitation method, and discussed the effects of solvent, stabilizer, volume ratio of organic phase to aqueous phase and drug concentration in organic phase upon particle size. Tozuka et al[29] gained indomethacin nanocrystals with stable particle size by supercritical fluid technology and investigated the effects of different factors on product quality. Recently, there has emerged a combination of the two methods. Wang et al[30] prepared glabridin nanosuspension by anti-solvent precipitation combined with homogenization method; Li et al[31] prepared ursodeoxycholic acid nanosuspension using high-pressure precipitation tandem homogenization technology, which was subsequently solidified through freeze-drying technology.

Hot Melt Extrusion (HME) technology utilizes temperature and mechanical energy to process the drug-excipient mixtures, and then extrudes them through a required mold.[32–34] Compared with traditional preparation technology, HME technology provides some advantages, such as simplifying the preparation process, enabling continuous operation and facilitating industrial production. In addition, it exhibits the benefits of being solvent-free and having good content uniformity.[35,36] HME has been developed extensively in past decades for its applications in taste masking,[32,37] improving the solubility and bioavailability of insoluble drugs.[38,39] With the use of this technique, a number of poorly soluble drugs, including Ritonavir (Norvir ®), Itraconazole (Onmel ®), Fenofibrate (Fenoglide ®), and Nifedipine (Adalat SL®), have

been successfully marketed,[38,40] the majority of which are amorphous solid dispersions. Furthermore, there exist reports about the preparation of nanocrystalline solid dispersion using hot melt extruder. The preparation process can be summarized as obtaining nanocrystalline suspension through the top-down process, then pouring the suspension into the hot melt extruder loaded with polymer (such as Soluplus and Hydroxypropyl cellulose), and removing the medium during the transfer process to finally acquire nanocrystalline solid dispersion.[40–43]

Our research group has discovered a new way to prepare nanocrystals directly by hot melt extruder without curing. Some insoluble drugs could be extruded with specific carriers at a temperature far below the melting point of drugs to obtain nanocrystals (also referred to nanocrystalline solid dispersion, nanocrystals are the term used in this paper since the crystal particle size is nanometer), which obviously improve the dissolution performance of drugs in vitro and absorption in vivo.

In this work, a twin-screw hot-melt extruder was employed to produce Cur-NCs with different drug loading utilizing EEP as the carrier. The morphology, particle size, melting point, and crystal structure of Cur in the extrudates were characterized by scanning electron microscope (SEM), dynamic light scattering (DLS), differential scanning calorimetry (DSC) and powder X-ray diffraction (PXRD). To confirm that the performances of Cur-NCs have been improved, tests on stability, wettability and sedimentation, dissolution in vitro, and absorption in vivo were also conducted. In the end, the mechanism of HME for successfully preparation of nanocrystals in a single step was briefly discussed.

Materials and Methods

Materials

Cur (≥95% purity, melting point 183 °C), hydrochloric acid, and anhydrous citric acid were purchased from Titan (Shanghai, China). Tween 80 was supplied by Damao (Tianjin, China). Eudragit ® EPO was obtained from Evonik (Essen, Germany). Emodin was sourced from McLean (Shanghai, China). β-glucosidase was supplied by Merck (Darmstadt, Germany). Acetic acid was received from Komio (Tianjin, China, chromatographic grade). Acetonitrile was purchased from Tedia (Ohio, USA, chromatographic grade) and methanol was purchased from Merck (New Jersey, USA, chromatographic grade). Water used throughout the study was deionized.

Preparation of Cur-NCs

The Cur-NCs employing EEP as the carrier were prepared by a twin-screw hot melt extruder (Mini CTW, Thermo Fisher, Germany) at the drug-carrier ratios of 1:1, 2:1, and 4:1. Briefly, the mixtures of Cur and EEP were introduced into the hot melt extruder and subjected to appropriate extrusion temperature and rotation speed. After cooling, the extruded strips were crushed and screened using an 80-mesh filter to acquire extrudate powder samples for further study.

Thermogravimetric Analysis (TGA)

The thermal stability of Cur was assessed by a TGA study (TGA/DSC 3+, Mettler Toledo, Switzerland). Placed Cur in an open aluminum pan and then heated from room temperature to 340 °C at a rate of 10 °C/min, air was used as the purge gas at a flow rate of 50 mL/min, data were collected to draw a weight-temperature curve.

Dynamic Light Scattering (DLS)

The extrudate powders or the corresponding physical mixtures (PMs) containing 25 mg of Cur were weighed and stirred in 10 mL of 0.1 M hydrochloric acid (HCl) solution to ensure that the carrier was completely dissolved and the drug was evenly dispersed. The particle size distributions of Cur dispersed in suspensions were measured by DLS (Delsa Nano laser particle size analyzer, Beckman, Germany). Set the temperature of the sample cell to 25 °C, and to ensure the accuracy of the determination results, the scattering strength of the sample should be controlled between 10,000 and 50,000 cps. The software would provide the distribution results of intensity, volume and number distribution after 70 consecutive measurements of each sample, which would also calculate the average diameter and Polydispersity Index (PDI).

Scanning Electron Microscope (SEM)

Cur and extruded samples were placed on the conductive adhesive, the powder on the surface was gently blown off and then gold was sprayed for 120 s in vacuum. The surface morphology of the sample was observed by SEM (HITACHI Regulus 8100, Hitachi, Tokyo, Japan) at an accelerated voltage of 5~10 kV. Along with this, we also observed the particle size and morphology of Cur in the extrudate filter residue. The extrudate powder was uniformly dispersed in a 0.1 M HCl solution, fully stirred to dissolve the carrier, then filtered with a 0.22 μm microporous membrane. The filter residue was dried in vacuum and then observed by SEM.

Differential Scanning Calorimetry (DSC)

The thermal behavior of the samples was examined through DSC (DSC250, Thermal, USA), which involved primary heating to identify the melting point and secondary heating to determine the glass transition temperature (Tg). 3~5 mg of the sample was sealed in an aluminum crucible and endured one or two heating processes. For first heating: the sample was heated from 40 °C to 200 °C at a speed of 10 °C/min; for secondary heating: after reaching 200 °C, the final temperature was kept for 5 min to ensure that the sample was completely melted, and then the temperature was rapidly lowered to -20 °C at a speed of 200 °C/min, maintained the final temperature for 5 min, and then raised to 200 °C at a rate of 20 °C/min. The determination process was protected by N_2 with the flow rate of 50 mL/min.

Powder X-Ray Diffraction (PXRD)

The crystalline state of the drug was characterized by PXRD (D/max-ultima iv x-ray diffractometer, Rigaku, Japan) to confirm whether there was crystal form transition during extrusion and stability study. Appropriate amounts of Cur, EEP and extrudate powder were respectively weighed and tested under the following conditions: target, Cu; voltage, 40 kV; current, 40 mA; diffraction angle range, 5~60 °; step size, 0.02 °; and scanning speed, 20 °/min.

Powder Dissolution

Powder dissolution was tested using an Intelligent Dissolution Instrument (ZRS-8GD, Tiandatianfa, Tianjin, China). Samples equivalent to 30 mg of Cur were poured into 900 mL of 0.1 M HCl solution containing 2% Tween 80. The temperature was set at 37.0 ± 0.5 °C and the paddle speed at 100 rpm. 5 mL dissolution media was withdrawn from each vessel at predetermined time intervals (2, 5, 10, 15, 30, 45, and 60 min) and supplemented with the same volume of fresh media to ensure a constant volume. A 0.22 μm filter membrane was used to filter the sample solution, and the first 2 mL of filtrate was discarded. The remaining filtrate was collected and then diluted to an appropriate concentration before detecting by UV-vis spectrophotometry (TU1900, General Analysis, Beijing, China) at 430 nm. The drug concentration was calculated according to the calibration curve. Each experiment was repeated in triplicate.

Intrinsic Dissolution Rate (IDR)

The IDR of the extrudate powder was determined by the rotating-disk method using an ultraviolet-visible spectrometer with optical fiber probe (AvaSpec-ULS2048CL, Avantes, Netherlands). 200 mg of sample was poured into an 8 mm-diameter mold and then compressed into a tablet. The IDR was determined by immersing the tablet-loaded mold, which was rotating at 240 rpm, into a 900 mL of 0.1 M HCl solution containing 2% Tween 80 at a temperature of 37.0 ± 0.5 °C. The optical fiber probe was used to measure the absorbance at 465 nm in real time, and the drug concentration was determined by the calibration curve before calculating the IDR of the sample. Each experiment was repeated in triplicate.

Stability Study

Considering that the sample may become unstable with the decrease of carrier content, the stability of the extrudate powder with the drug-carrier ratio of 4:1 was tested by aluminum foil bag packaging at 40 °C and 75% humidity. In addition to observing the characteristics of the sample, partial samples were taken out at 0, 1, 2, and 3 months respectively to analyze the content, powder dissolution, DSC and PXRD.

Pharmacokinetics in vivo

Healthy male Sprague-Dawley rats (220~250 g), which were purchased from the Experimental Animal Center of Zhejiang Academy of Medical Sciences, were used for pharmacokinetics studies. All the animals were fed a regular diet and acclimatized for 1-week prior to the experiment. Each experimental procedure had been reviewed and approved by the Ethics Committee of Animal Experimental Center of Zhejiang University of Technology, and it was in line with Laboratory animals-General code of animal welfare (GB/T42011-2022) of People's Republic of China standards.

Ten SD rats were randomly divided into two groups of five rats each. Pure Cur and Cur-NCs were dispersed in 0.1 M citric acid to prepare the suspension containing 60 mg/mL Cur. Rats were fasted but allowed to drink freely for 12 h before oral administration at a single dose of 200 mg/kg. At predetermined intervals of 0.33, 0.67, 1, 1.5, 2, 3, 4, 6, 8, 12, and 24 h, about 0.5 mL of blood was collected from the orbital vein into an anticoagulation EP tube. Plasma was obtained by centrifugation at 4000 rpm under 4 °C for 10 min.

As for the treatment of samples, a 200 μL plasma sample was added with 10 μL of 30 μg/mL emodin internal standard solution and 1 mL of acetonitrile to precipitate protein. The mixture was vortexed for 3 min and centrifuged for 10 min at 10,000 rpm. The solvent was removed with nitrogen blowing at 40 °C, after then 100 μL of mobile phase (Acetonitrile: 5% acetic acid aqueous solution = 50:50) was added to dissolve the sample, vortexed 15 s, and centrifuged (10,000 rpm×10 min). The supernatant was detected by HPLC (LC1260, Agilent, America) under the following conditions: Column: HypersilODS2 C18 column (5 μm, 4.6 mm×250 mm), at a temperature of 30 °C; UV detection at 430 nm; A gradient mobile phase consisting of acetonitrile (A) and 5% acetic acid aqueous solution (B) at a flow rate of 1 mL/min, and the gradient conditions of mobile phase were 0 ~ 6 min: 40% ~65% A; 6 ~ 15 min: 65%A; 15 ~ 15.5 min: 65% ~40% A; and finally 15.5 ~ 20 min: 40%A, which was used to reestablish equilibrium before sample injection. It was found the linear range of 0.05 ~ 20.0 μg/mL, with a detection limit of 0.025 μg/mL, a quantitative limit of 0.05 μg/mL and a retention time of 8.5 min. Finally, the pharmacokinetic parameters were calculated by DAS2.0 software.

Results and Discussion

Characterization of Cur-NCs

A preliminary screening process was carried out to find carriers that can be co-extruded with Cur to obtain nanocrystals. Various carriers such as EEP, Polyvinylpyrrolidone K30 (PVP K30), polyvinylpyrrolidone (VA64), Hydroxypropyl methyl-cellulose E5 (HPMC E5), and Polyethylene Glycol 6000 (PEG 6000) were extruded separately with Cur at the ratio of 1:1, the screw speed was 30 rpm and the operating temperature was kept as low as possible to maintain the torque within the capacity of the machine, after which the particle sizes of Cur dispersed in the extrudates were characterized by DLS. It was found that only EEP could be used to successfully prepare Cur-NCs, and the sieved particles were observed to have good fluidity, which was benefit for the development of downstream processes and had strong industrial applicability. So EEP was selected as the carrier, and the drug loading was investigated with drug-carrier ratios of 1:1, 2:1, 4:1 and 6:1, which were extruded at 90 °C, 105 °C, 125 °C and 135 °C respectively. It could be found that the temperature required for preparation increased correspondingly with the increase of drug loading. The particle size of Cur dispersed in the products was determined by DLS after adding products into hydrochloric acid solution to dissolve the carrier completely. The results are shown in Figure 1, from which we could see that the dispersion size of Cur in the extruded sample with the drug-carrier ratio of 1:1 was the smallest, which was only 56 nm, with a narrow particle size distribution. Samples with the drug-carrier ratios of 2:1 and 4:1 produced similar results with the dispersed size of 146 nm and 137 nm separately, while the dispersed size of the sample with the ratio of 6:1 was 1101 nm and had a wide distribution. The large particles in the suspension were scattered immediately when treated with ultrasonic, which indicated that it was difficult for water to enter the highly hydrophobic drug gap to dissolve the carrier and release the drug due to the decrease of the carrier, thus losing the advantages of nanocrystals. To sum up, nano-sized Cur could be prepared by the optimized HME process.

The state of drugs in the extrudates was analysis by DSC and PXRD. The melting points shown in the DSC diagram (Figure 2A) were close to those reported in the literature,[44–47] in which the melting point of pure Cur was 183.5 °C, while the extruded sample moved to the left with the increase of carrier content, in the behavior of melting depression.[48] PXRD pattern (Figure 2B) showed that the major characteristic peaks of pure Cur were 8.90, 12.26, 14.54, 17.24, 23.33, 24.60,

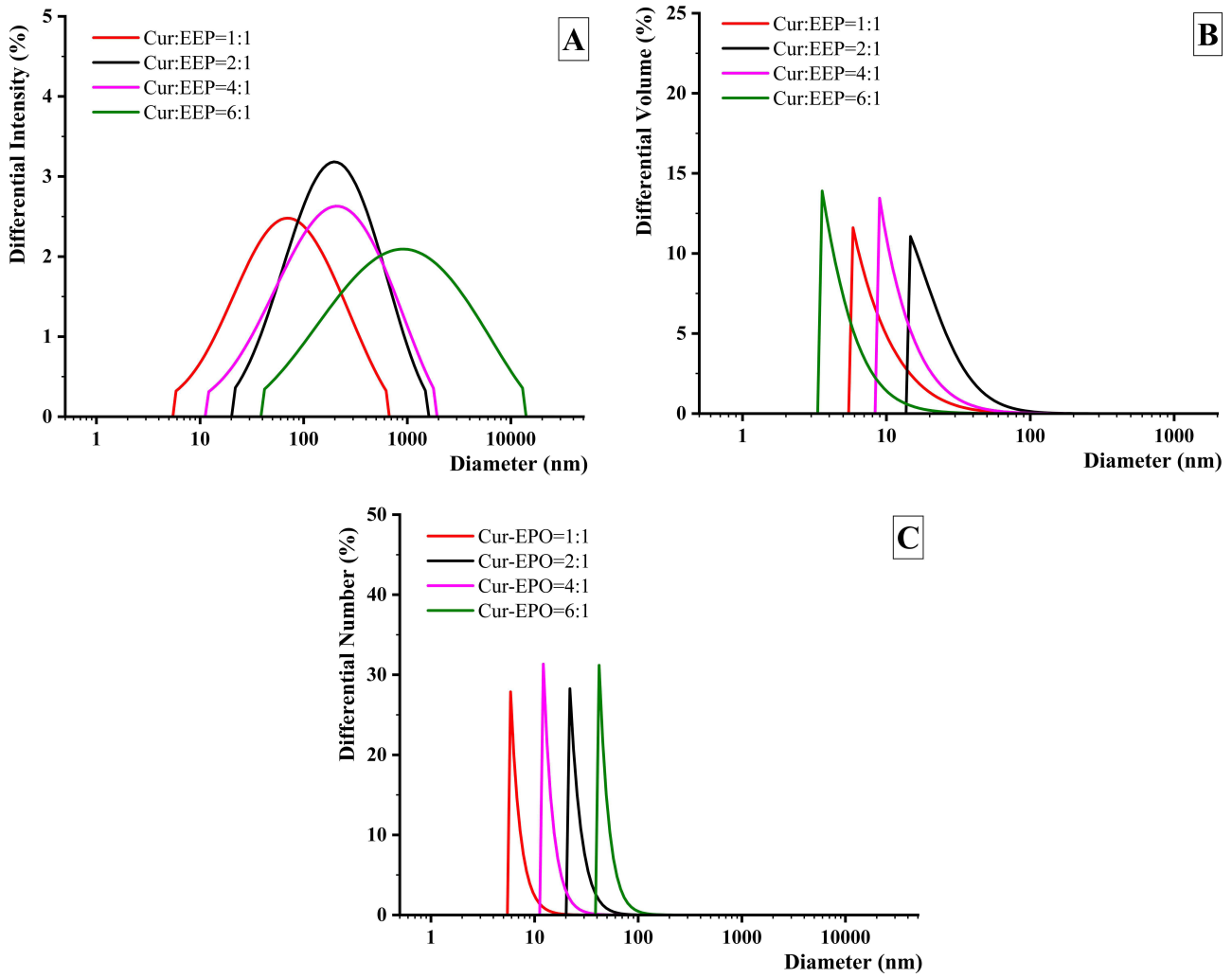

Figure 1 The particle size distribution results of Cur in extrudates include (**A**) Intensity Distribution, (**B**) Volume Distribution, (**C**) Number Distribution.
Notes: The particle distributions shown were determined using a laser diffraction particle size analyzer (Delsa Nano, Beckman, Germany).
Abbreviations: Cur, curcumin; EEP, Eudragit® EPO.

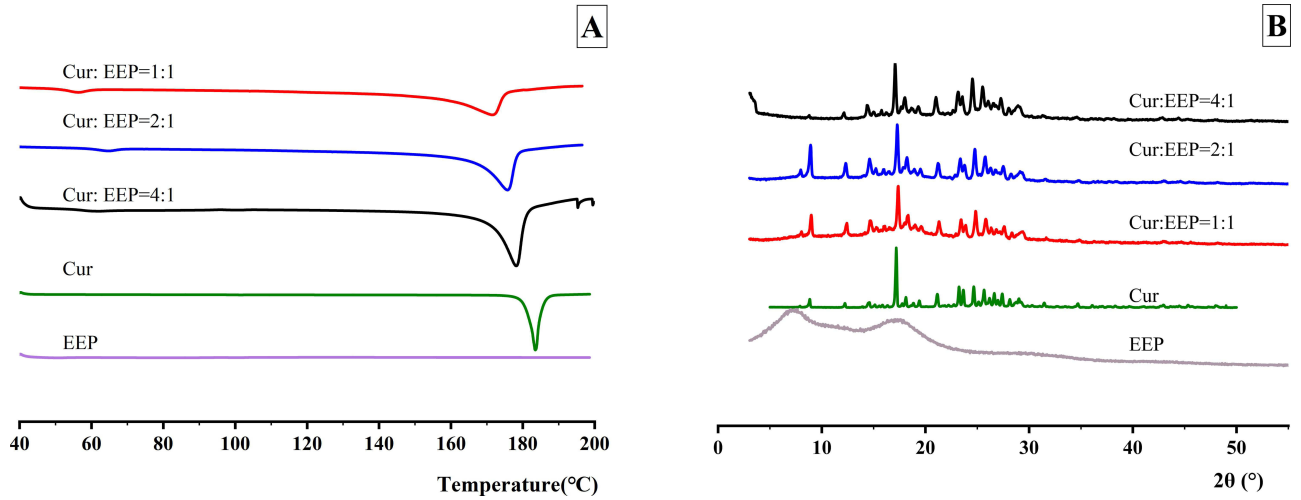

Figure 2 (**A**) DSC and (**B**) PXRD diagrams of Cur, EEP, and Cur-NCs with different drug loading.
Abbreviations: Cur, curcumin; EEP, Eudragit® EPO; DSC, differential scanning calorimetry; PXRD, powder X-ray diffraction.

and 25.52°,[49] indicating the solid state of the Cur was a relatively stable crystal form 1.[14,45,50,51] There was no significant change in the position and shape of the peaks of the extruded powders with different drug loadings, indicating that the crystal form did not change either before or after extrusion. Therefore, it was obvious that Cur still existed in crystalline form even after extrusion by hot melt process.

The dispersion states of pure Cur, PM, and extrudate powders in hydrochloric acid medium were observed to compare the wettability (Figure 3A) and sedimentation (Figure 3B). After fully shaking and mixing, all three samples could be evenly dispersed in the medium. Different from Cur and PM with small solid particles in suspension, there were no obvious particles in extrudate suspension, and the color of the extrudate suspension changed to a brilliant yellow, which might have resulted from the fluorescence induced by Cur or the nano-sized particles. After standing for 12 h, the pure Cur and the mixture were partially or completely settled while the extrudate still suspended very well, indicating that size of Cur was reduced significantly after extrusion. Judging from the color of the supernatant, Cur did hardly dissolve.

The morphology and particle size of pure Cur and extruded samples were observed by SEM. The results showed that pure Cur (Figure 4A) was micron-sized with regular crystal characteristics, and the particle size of the extruded powder (Figure 4B) was decreased to nano-sized and was closely arranged. After removing the carrier of the extruded powders with hydrochloric acid medium, the filter residue (Figure 4C), instead of a regular crystal shape of Cur, was irregular with nano size, which is consistent with the dispersion size measurement results.

Thermostability

As a polyphenol compound,[4,9] the thermal stability of Cur in weakly acidic or neutral environment will be greatly reduced.[52] Since heating is essential in the hot melt extrusion process, and the high temperature experienced for the drug and carrier during HME, which may result in the occurrence of degradation, thermally induced chemical reactions, or both,[36] so it is necessary to conduct TGA analysis of Cur prior to HME. Air was utilized as purge gas throughout the detection process, which increased the contact between Cur and oxygen to enhance their interaction. TGA diagram (Figure 5) shows that the degradation temperature of Cur was about 250 °C, which was consistent with the literature.[46,53,54]

The extrusion process is more complicated than TGA detection process, so we investigated the influence of extrusion temperature on the content of Cur, which was detected by HPLC under the same conditions as the pharmacokinetic study. It was found that when the extrusion temperature was 175 °C, the extrudate turned purple-black with the content dropped to 41.0%, and there were obvious impurity peaks on the chromatogram graph (not shown). After turning the extrusion temperature down to 150 °C, the sample was brown and the content decreased slightly to 94.1%. However, when the extrusion temperature was 135 °C, the content of extrudate was 100.3%. Therefore, we suggest that the extrusion temperature of Cur and EEP should be as low as possible, and the highest allowable temperature should not exceed 135 °C to minimize the possibility of thermal degradation of Cur during extrusion.

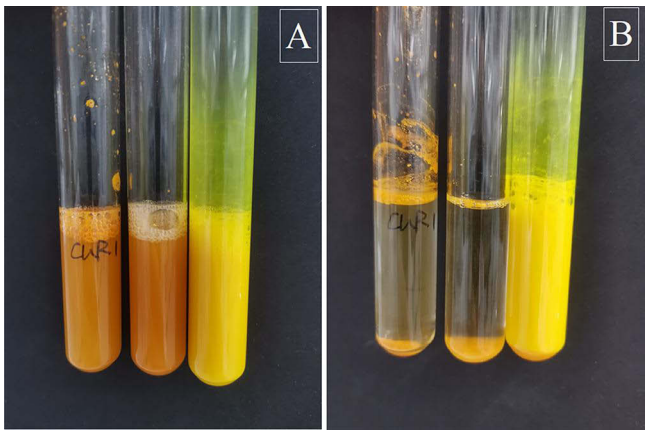

Figure 3 The wettability (**A**) and sedimentation (**B**) of samples.
Notes: From the left to the right side of each picture were Cur, Cur-EEP=1:1 (PM), Cur-EEP =1:1 (NC).
Abbreviations: Cur, curcumin; EEP, Eudragit® EPO; PM, physical mixture; NC, nanocrystal.

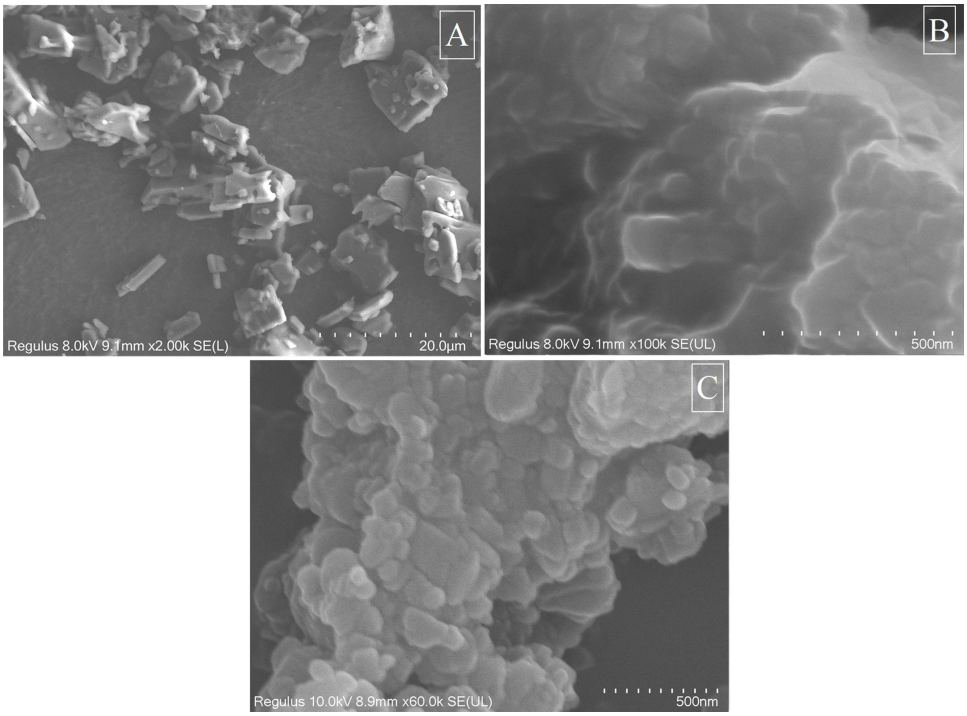

Figure 4 SEM micrographs of (**A**) Cur, (**B**) Extruded sample and (**C**) Filter residue of the extrudate with drug-carrier ratio of 4: 1.
Notes: In order to obtain filter residue, the carrier in the extrudate powder was dissolved by 0.1 M HCl solution, followed by filtering and drying.
Abbreviations: SEM, scanning electron microscope; Cur, curcumin.

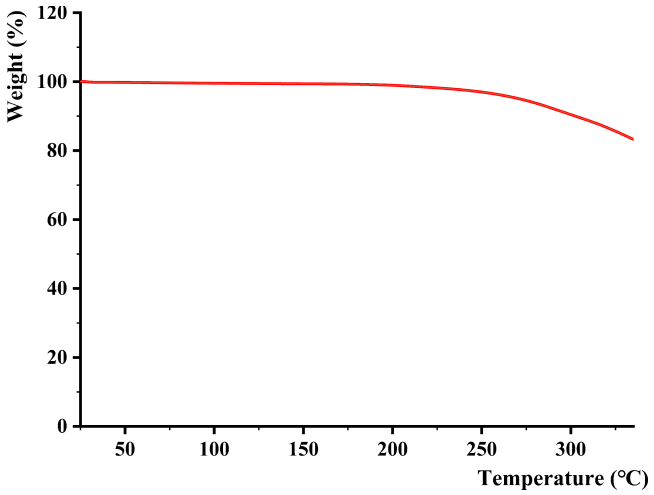

Figure 5 TGA diagram of Cur.
Abbreviations: TGA, Thermogravimetric analysis; Cur, curcumin.

Powder Dissolution

Powder dissolution test is a classic method for evaluating solubilization effect, so a standard dissolution method of USP type II apparatus was carried out to demonstrate the dissolution enhancement of Cur-NCs. Since the pH depended solubility of the carrier EEP and the extremely low solubility of Cur, an acidic medium was used with an additional 2% Tween 80 to prevent the interference of the carrier and guarantee the sink condition during the dissolution of Cur, and the results are shown in Figure 6. Either pure Cur or the mixture of Cur and EEP dissolved slowly with the cumulative dissolution percentage of nearly 80% in 60 min, indicating that the EEP did not have a solubilizing effect. As for the

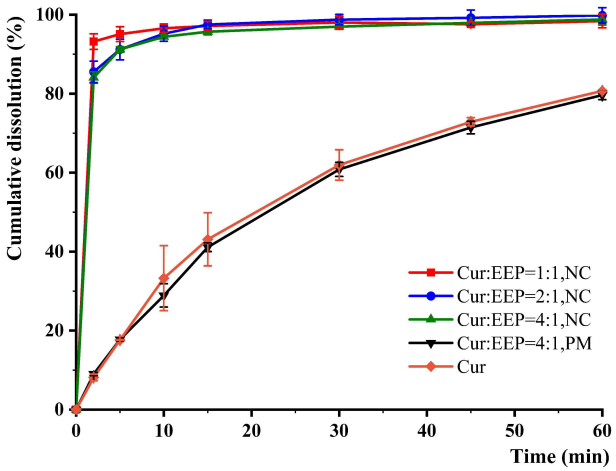

Figure 6 Powder dissolution curves of Cur-NCs with different drug loading.
Note: The experiment was performed in triplicate.
Abbreviations: Cur, curcumin; EEP, Eudragit® EPO; NC, nanocrystal; PM, physical mixture; Cur-NCs, curcumin nanocrystals.

extruded samples, the dissolution percentage of all the three extrudates could reach 80% in less than 2 min. This might be due to the drug with extremely small particle size dispersed uniformly in the carrier, and huge specific surface area would be produced once the carrier contacted the medium and dissolved quickly. Additionally, it was observed that the sample with 50% drug loading dissolved more rapidly in 2 and 5 min compared to the other two samples at the same dosage, suggesting that with the increase of drug loading, the hydrophilicity of EEP deteriorated, resulting in a slight decrease of dissolution rate.

Intrinsic Dissolution Rate (IDR)

Due to the huge surface area of drug particles, the powder of extrudates dissolved very quickly, so the difference of powder dissolution rates of the extrudates with various drug loadings was insignificant. Therefore, IDR tests with fixed dissolving area were carried out, and the results are shown in Figure 7. The dissolution of Cur was extremely slow, which got an IDR of 0.04 ± 0.00 mg/min/cm^2, and the color of the medium did not change obviously after testing (Figure 8A). After extruded with EEP to get Cur-NCs, the dissolution rates were improved dramatically. Through the normalization of

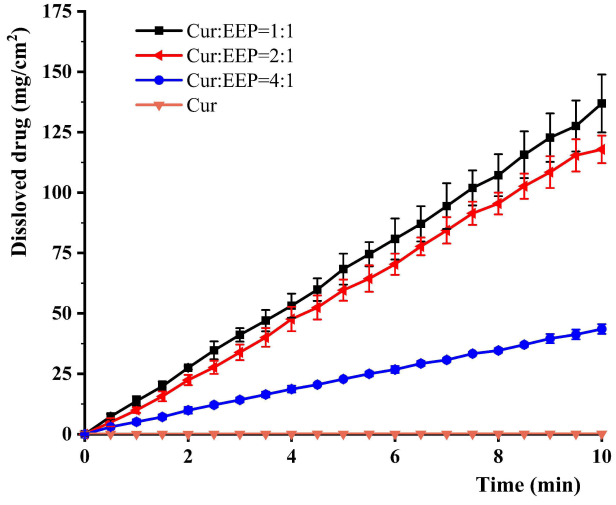

Figure 7 Intrinsic dissolution curves of Cur-NCs with different drug loading.
Note: The experiment was performed in triplicate.
Abbreviations: Cur, curcumin; EEP, Eudragit® EPO; Cur-NCs, curcumin nanocrystals.

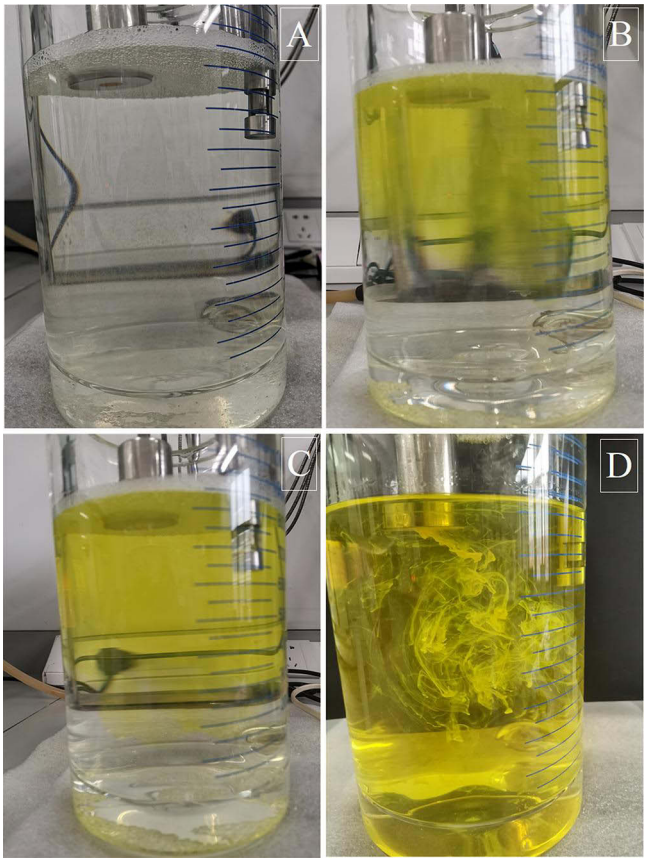

Figure 8 Photos taken from IDR test.
Notes: (**A**) was taken at the end of pure Cur IDR test; (**B**) and (**C**) were taken a few seconds after the start of the IDR test of Cur-NCs; (**D**) was taken when the rotation speed was kept at 0rpm of Cur-NC.
Abbreviations: IDR, intrinsic dissolution rate; Cur, curcumin; Cur-NC, curcumin nanocrystal.

Cur dissolution area, the IDR results of the extruded samples with drug-carrier ratios of 1:1, 2:1 and 4:1 were 13.68 ± 1.20 mg/min/cm^2, 11.78 ± 0.57 mg/min/cm^2, and 4.35 ± 0.20 mg/min/cm^2, respectively, which decreased with the increase of drug loading. It could be observed that the medium turned yellow rapidly from top to bottom within a few seconds once the tablet contacted the medium (Figure 8B and C). Furthermore, an interesting "smoking" phenomenon was observed when the rotating speed was zero (Figure 8D). It was because the large number of nanosized Cur was released by the rapid dissolution of the carrier, a part of which dissolved immediately and formed a local saturated solution, and the remaining particles that could not be dissolved in time diffused and then dissolved under various interaction forces, such as van der Waals force, hydrophobic interaction, electrostatic interaction, hydrogen bonding and Brownian motion.[55] Therefore, the "smoke" we saw was denser near the tablet while it was filamentous in the distance, and the color of the medium turned yellow gradually with time.

Stability Study

Unlike amorphous solid dispersions which would lose enthalpy, entropy and free energy, they tend to convert back to their stable crystalline form over time.[33,47,56] The stability of the nanocrystalline solid dispersion we prepared is good in theory, in which the drug particles were uniformly dispersed in the carrier in the form of crystals. In order to verify this, the stability research was carried out, and the results showed that the content (Table 1) and the dissolution performance (Figure 9A) of Cur-NCs did not change significantly during the whole three-month accelerated test. Besides, the melting point peak of the drug in DSC (Figure 9B) and the position and shape of its characteristic peaks in PXRD (Figure 9C) remained almost unchanged, showing the good stability of the prepared Cur-NCs.

Table 1 Assay Results of 0~3 M for Cur-NC Powders with Drug-Carrier Ratio of 4:1 in Stability Study

Time	Assay %, Mean ± SD
0 M	101.9% ± 1.1%
1 M	98.6% ± 1.8%
2 M	97.2% ± 0.5%
3 M	99.2% ± 0.7%

Note: Data were represented as mean ± SD (n=3).
Abbreviations: M, month; Cur-NCs, curcumin nanocrystals.

Pharmacokinetics in vivo

Despite its valuable medicinal properties, Cur's practical application is restricted due to its low solubility, poor absorption in the gastrointestinal tract, rapid metabolism and low bioavailability in vivo.[47] Recently, nanocrystals have received increasing

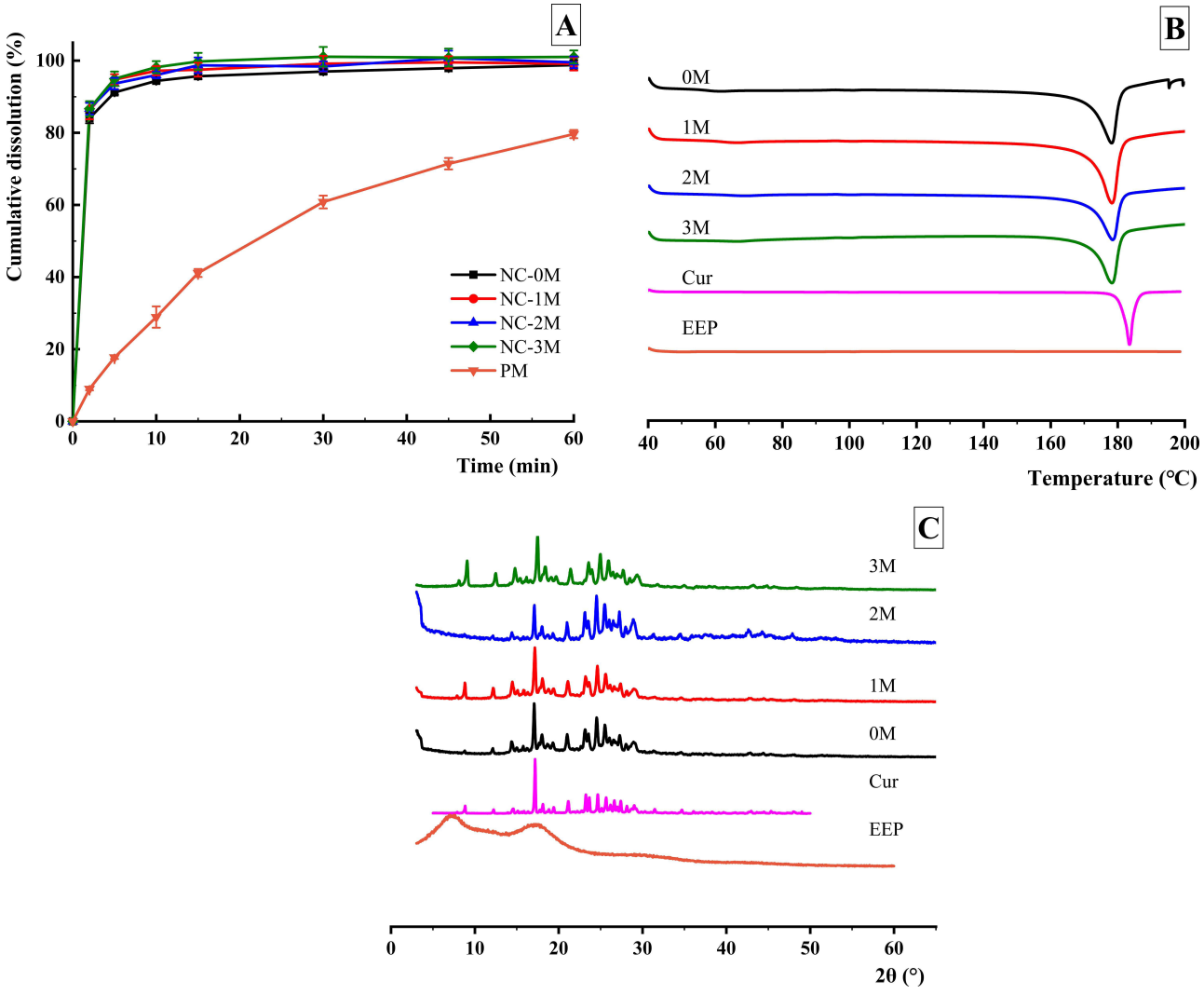

Figure 9 (**A**) Powder dissolution curves, (**B**) DSC, (**C**) PXRD of Cur-NC for 0~3 months in the stability study.
Notes: The drug-carrier ratio of Cur-NCs was 4: 1. Samples were packed in aluminum foil bags and tested at 40°C and 75% humidity.
Abbreviations: NC, nanocrystal; M, month; PM, physical mixture; Cur, curcumin; EEP, Eudragit® EPO.

attention because they are one of the most promising strategies in improving the oral bioavailability of insoluble drugs.[15,16,47,57,58] Therefore, animal experiments were conducted to determine whether the prepared Cur-NCs improved the bioavailability. The preliminary-experiment revealed that although the color of some treated plasma samples of the group of Cur-NC was yellow, the concentration of Cur was extremely low. And there was a significant chromatographic peak at 4.5 min except Cur and internal standard substance, suggesting the yellow substances were mainly metabolites of Cur.[59] To identify the metabolites, we treated the plasma samples with β-glucosidase, and found the peak area of Cur considerably increased, indicating that the metabolites were glucosides of Cur. Moreover, with the increase of enzyme dosage, the ratio of the metabolites peak area decrement to the Cur peak area increment was close to 1 (Table S1 and Figure S1). So the concentrations of both prototype and the metabolites of Cur in plasma samples were determined simultaneously by HPLC, and the concentration of the metabolites was calculated using the conversion factor of 1.

Owing to the rapid metabolism of Cur in vivo, it could be seen that the C_{max} (Figure 10A) of the prototype in Cur-NC group was 103.588 ± 12.275 ng/mL, which was 1.68 times higher than that of pure Cur group (61.532 ± 25.619 ng/mL, $p<0.05$). The drug concentration in the Cur-NC group was generally higher than those of pure Cur group, but the errors of concentration at each time point were relatively large. Besides the individual error of rats, it may also be due to the detection sensitivity of HPLC was not high enough, and the data below the quantitative limit (as mentioned above, 0.05 μg/mL) were included in the calculation without being excluded. As for metabolites (Figure 10B), it could be found that the concentration of metabolites in plasma was significantly higher than that in prototype regardless of the Cur group or the Cur-NC group. The metabolites concentration in the Cur-NC group, for example, was 232.50 ng/mL at the first time point of 20 min, while the prototype was 59.34 ng/mL. Correspondingly, the Cur group were 51.03 ng/mL and 57.93 ng/mL, which meant that the plasma exposures of Cur (the sum of prototype and metabolites) were 291.84 ng/mL and 108.96 ng/mL, respectively, and the former was 2.68 times that of the latter. Overall, the C_{max} and $AUC_{0-\infty}$ of metabolites in Cur-NC group were 2.79 times and 4.07 times higher than those of Cur group (Table 2), indicating that there was a considerable increase in the absorption of Cur-NC.

There were two peaks in each concentration-time curve, which might be the result of enterohepatic circulation, that is, metabolites entered the small intestine with bile, after which were hydrolyzed and reabsorbed.[60] The C_{max} of Cur-NC prepared by Wang et al[57] using high-pressure homogenization process was 27.95 ± 2.50 ng/mL, and the enterohepatic circulation also occurred. Pharmacokinetic parameters showed that the mean retention time (MRT) of Cur-NC group was longer than that of Cur group, and the drug concentration in the curve could be maintained at a high level for a long time. This was probably due to the adhesion of gastrointestinal mucosa to nano-drug particles that prolonged the retention time of drug particles in the gastrointestinal tract, and the continuous dissolution of drug particles generated a high

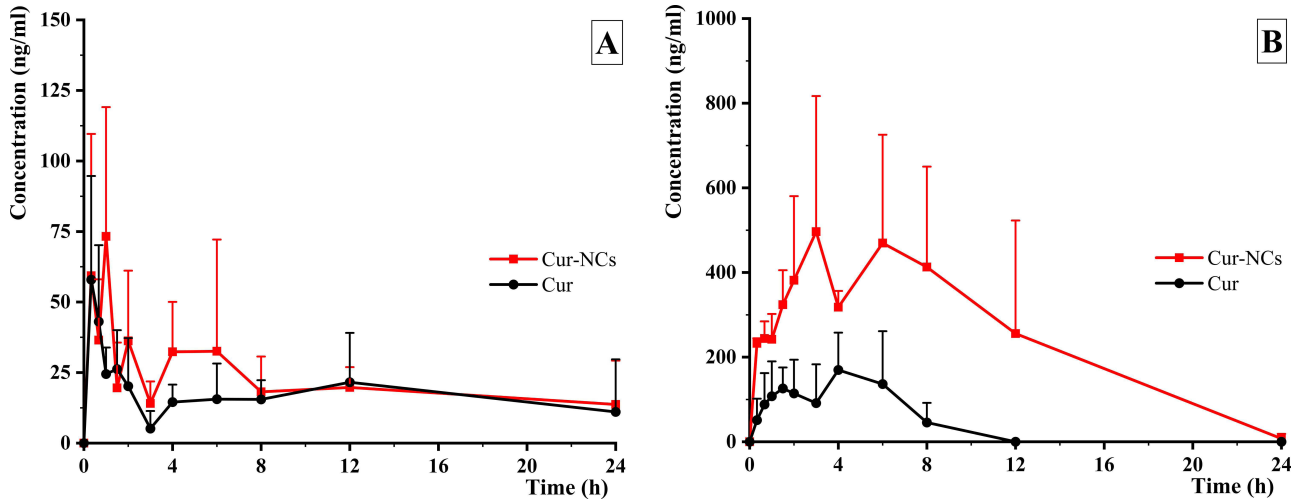

Figure 10 The plasma concentrations versus time curves of (**A**) Prototype and (**B**) Metabolites of Cur after oral administration in rats. ($\bar{x} \pm s$, n = 5).
Notes: The pharmacokinetic parameters are shown in Table 2. Rats were treated with Cur (200 mg/kg) or Cur-NCs (equivalent to the Cur).
Abbreviations: Cur-NCs, curcumin nanocrystals; Cur, curcumin.

Table 2 Pharmacokinetic Parameters of Cur Metabolites in Plasma After Oral Administration

Pharmacokinetic Parameters	Cur-NCs	Cur
t_{max} (h)	5.800 ± 4.087	3.334 ± 2.054
$t_{1/2}$ (h)	2.700 ± 0.807	1.919 ± 3.601
C_{max} (ng/mL)	621.298 ± 209.060**	222.366 ± 72.149
AUC_{0-t} (ng/mL*h)	5215.565 ± 3273.311*	1174.247 ± 444.205
$AUC_{0-\infty}$ (ng/mL*h)	5900.697 ±2856.408*	1451.529 ± 680.295
MRT_{0-t} (h)	6.090 ± 1.891	4.143 ± 0.526
$MRT_{0-\infty}$ (h)	7.008 ± 1.807	6.040 ± 4.001

Notes: Data were represented as mean ± SD (n=5). Compared with Cur, *P<0.05, **P<0.01.
Abbreviations: Cur, curcumin; Cur-NCs, curcumin nanocrystals; t_{max}, time at peak concentration; $t_{1/2}$, terminal elimination half-life; C_{max}, peak plasma concentration; AUC, area under the curve; MRT, mean retention time.

concentration gradient, which was conducive to the absorption of drug.[21,23,61,62] It is also worth mentioning that the steady blood concentration provides the feasibility for reducing the dosage and frequency of administration.

Formation Mechanism of Nanocrystals

Although HME has been used in pharmaceuticals for decades, its use to prepare drug nanocrystals is less common. Our research group has successfully prepared carbamazepine and piroxicam nanocrystals using HME.[63,64] As the results presented in this work, Cur-NCs were also prepared by the HME process. However, the exactly formation mechanism of nanocrystals by HME was not clear. We think it can be explained through both top-down techniques and bottom-up techniques.

Top-down techniques, for example, can be interpreted as that drugs are crushed into small particles by mechanical forces such as compressive and shear forces by the twin screws in the process of mixing and transferring with carriers in the hot melt extruder. Herein, we believe that raw materials with strong brittleness are conducive to reaching nano-size. In addition, the lowest possible temperature during extrusion is beneficial to maintain brittle characteristics of the drug, and carriers in this condition usually exhibit high viscosity, which contributes to the transmission of mechanical force. Apart from this, the fluidity of the carrier makes it much easier to mix the physical mixture evenly, which contributes to wrapping and isolating the drug nanoparticles to some extent. Based on this idea, our group had studied the properties of different drugs and carriers, for which certain requirements were put forward.[65]

As for bottom-up techniques, we believe that the polymer molecular chain can be fully stretched and interact with small molecular drug under the thermal and mechanical effects, such as shear thinning, which makes it possible for the drug to reach a molten or dissolved state at a temperature below or even far below the melting point, and subsequently forms a supersaturated drug-carrier solution. Owing to the changes of temperature and pressure, the molten or dissolved drug rapidly nucleates and grows in the solidification process of the carrier, and finally forms drug nanocrystals which are uniformly dispersed in the carrier. The whole process is probably not only related to the interaction between drug and carrier like the miscibility or solubility between them, but also related to the crystallization kinetics, such as the crystallization trend of drug. Xu et al[66] summarized the solubility parameters of Cur and EEP in several calculation methods and considered that they have good miscibility. On this basis, whether the intermolecular interaction existed between Cur and EEP was studied by measuring the glass transition temperature (Tg) values of physical mixtures with different proportions. The results showed that with the Cur content increased, the Tg values (Figure 11 and Table 3) shifted to the right and were consistently higher than the theoretical values calculated according to the Gordon-Taylor equation, which indicated that there was a strong intermolecular interaction between Cur and EEP.[67–70] However, the mixtures of Cur-PVP K30 and Cur-VA64 that cannot be extruded into nanocrystals showed weak intermolecular interaction, in which the Tg difference between the experimental

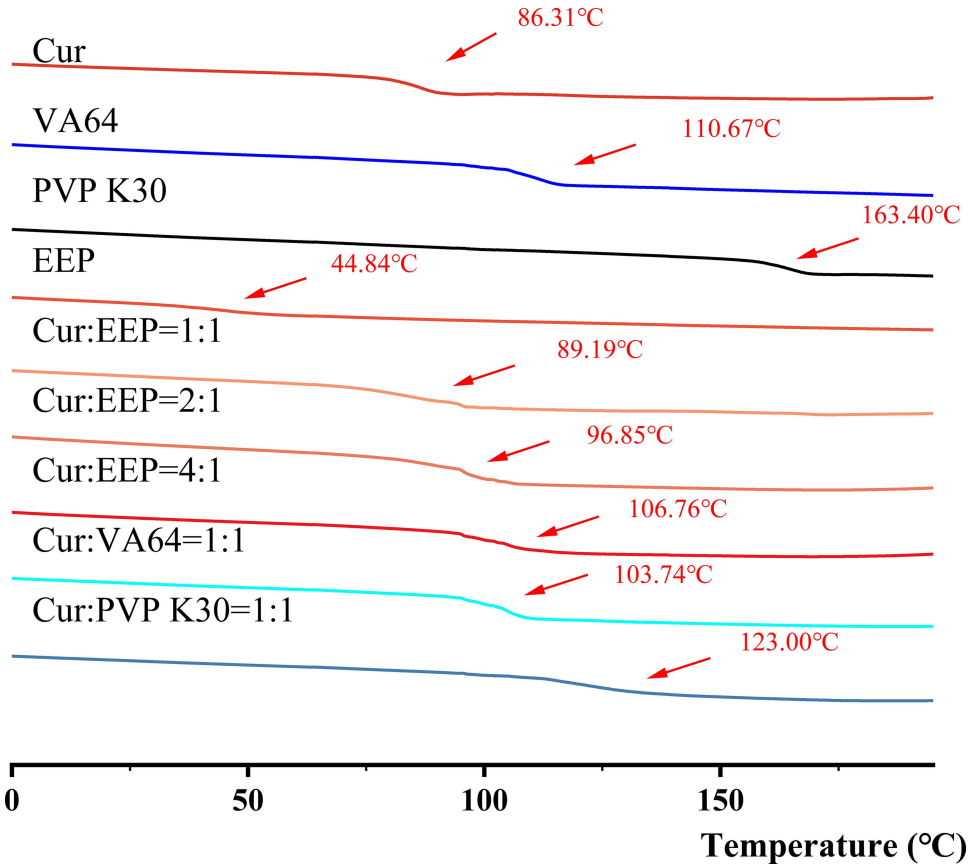

Figure 11 Experimental Tg values of Cur, EEP, VA64, PVP K30 and physical mixtures.
Notes: The experimental and theoretical Tg values of Cur, carriers, and PMs are shown in Table 3.
Abbreviations: Cur, curcumin; VA64, polyvinylpyrrolidone; PVP K30, Polyvinylpyrrolidone K30; EEP, Eudragit® EPO; Tg, the glass transition temperature.

value and the theoretical value of Cur-PVP K30 mixture was less than zero, while that of Cur-VA64 mixture was 4.89. The reason why HME technology successfully prepared drug nanocrystals in one step needs further study as both the above two explanations are reasonable at present.

Table 3 The Experimental and Theoretical Tg Values of Cur, Carriers, and PMs

Samples	Experimental Values of Tg (K)	Theoretical Values of Tg (K)	ΔTg (K)*
EEP	317.99	–	–
Cur	359.46	–	–
Cur-EEP=1-1, PM	362.34	335.97	26.37
Cur-EEP=2-1, PM	370.00	329.47	40.53
Cur-EEP=4-1, PM	379.91	349.25	30.66
PVP K30	436.55	–	–
Cur-PVP K30=1-1, PM	396.15	399.15	−3.00
VA64	383.82	–	–
Cur-VA64=1-1, PM	376.89	372.00	4.89

Note: *The experimental value minus the theoretical value.
Abbreviations: Tg, the glass transition temperature; Cur, curcumin; PM, physical mixture; EEP, Eudragit® EPO; PVP K30, Polyvinylpyrrolidone K30; VA64, polyvinylpyrrolidone.

Conclusion

In this study, Cur-NCs in solid state could be successfully prepared by Cur and EEP at suitable extrusion temperature and screw speed. Cur in the extrudate exhibited good stability in both preparation and storage, and the technology was simple, continuous, safe and environmentally friendly. As shown by the research results, the cumulative dissolution percentage of Cur-NCs could reach 80% within 2 min, and animal experiment showed that the AUC of metabolites in Cur-NC group was 4.07 times higher than that in Cur group, which laid a foundation for giving full play to the pharmacological activities of Cur. In summary, preparation of nanocrystals by HME technology in one-step provides a new idea for the development of insoluble pharmaceuticals, which has great research value and broad application prospects.

Acknowledgments

This work was supported by latitudinal projects (No.KYY-HX-20221151).

Disclosure

The authors report no conflicts of interest in this work.

References

1. Mondal S, Ghosh S, Moulik SP. Stability of curcumin in different solvent and solution media: UV–visible and steady-state fluorescence spectral study. *J Photochem Photobiol B*. 2016;158:212–218. doi:10.1016/j.jphotobiol.2016.03.004
2. Kanai M, Imaizumi A, Otsuka Y, et al. Dose-escalation and pharmacokinetic study of nanoparticle curcumin, a potential anticancer agent with improved bioavailability, in healthy human volunteers. *Cancer Chemother Pharmacol*. 2012;69(1):65–70. doi:10.1007/s00280-011-1673-1
3. Ak T, Gülçin I. Antioxidant and radical scavenging properties of curcumin. *Chem Biol Interact*. 2008;174(1):27–37. doi:10.1016/j.cbi.2008.05.003
4. Maiti K, Mukherjee K, Gantait A, Saha BP, Mukherjee PK. Curcumin-phospholipid complex: preparation, therapeutic evaluation and pharmacokinetic study in rats. *Int J Pharm*. 2007;330:155–163. doi:10.1016/j.ijpharm.2006.09.025
5. Fang M, Jin YL, Bao W, et al. In vitro characterization and in vivo evaluation of nanostructured lipid curcumin carriers for intragastric administration. *Int J Nanomed*. 2012;7:5395–5404. doi:10.2147/ijn.S36257
6. Meybodi SM, Rezaei P, Faraji N, et al. Curcumin and its novel formulations for the treatment of hepatocellular carcinoma: new trends and future perspectives in cancer therapy. *J Funct Foods*. 2023;108:105705. doi:10.1016/j.jff.2023.105705
7. Yallapu MM, Nagesh PKB, Jaggi M, Chauhan SC. Therapeutic Applications of Curcumin Nanoformulations. *AAPS J*. 2015;17(6):1341–1356. doi:10.1208/s12248-015-9811-z
8. Kumar R, Chauhan S. Cellulose nanocrystals based delivery vehicles for anticancer agent curcumin. *Int J Biol Macromol*. 2022;221:842–864. doi:10.1016/j.ijbiomac.2022.09.077
9. Yavarpour-Bali H, Ghasemi-Kasman M, Pirzadeh M. Curcumin-loaded nanoparticles: a novel therapeutic strategy in treatment of central nervous system disorders. *Int J Nanomed*. 2019;14:4449–4460. doi:10.2147/ijn.S208332
10. Bangphumi K, Kittiviriyakul C, Towiwat P, Rojsitthisak P, Khemawoot P. Pharmacokinetics of curcumin diethyl disuccinate, a prodrug of curcumin, in Wistar rats. *Eur J Drug Metabol Pharmacokinet*. 2016;64. doi:10.1016/j.jddst.2021.102564
11. Xiqin Z, Yuanyuan F, Jingjing L, Suning C. Pharmacological progress of curcumin nanoparticles against tumor of digestive system. *Drug Eval Res*. 2022;45(7):1440–1445. doi:10.7501/j.issn.1674-6376.2022.07.028
12. Huang S, Xu DD, Zhang L, et al. Therapeutic effects of curcumin liposomes and nanocrystals on inflammatory osteolysis: in vitro and in vivo comparative study. *Pharmacol Res*. 2023;192:106778. doi:10.1016/j.phrs.2023.106778
13. Yallapu MM, Jaggi M, Chauhan SC. Curcumin nanoformulations: a future nanomedicine for cancer. *Drug Discovery Today*. 2012;17(1–2):71–80. doi:10.1016/j.drudis.2011.09.009
14. Pantwalawalkar J, More H, Bhange D, Patil U, Jadhav N. Novel curcumin ascorbic acid cocrystal for improved solubility. *J Drug Deliv Sci Technol*. 2021;61:102233. doi:10.1016/j.jddst.2020.102233
15. Zhang J, Liang Y-C, Lin X, et al. Self-monitoring and self-delivery of photosensitizer-doped nanoparticles for highly effective combination cancer therapy in vitro and in vivo. *ACS nano*. 2015;9(10):9741–9756. doi:10.1021/acsnano.5b02513
16. Zhang J, Li S, F-f A, et al. Self-carried curcumin nanoparticles for in vitro and in vivo cancer therapy with real-time monitoring of drug release. *Nanoscale*. 2015;7(32):13503–13510. doi:10.1039/C5NR03259H
17. Xiang H, Xu S, Zhang WX, Li Y, Zhou YX, Miao XQ. Skin permeation of curcumin nanocrystals: effect of particle size, delivery vehicles, and permeation enhancer. *Colloids Surf B Biointerfaces*. 2023;224:113203. doi:10.1016/j.colsurfb.2023.113203
18. Lizonová D, Hládek F, Chvíla S, Baláz A, Stanková S, Stepánek F. Surface stabilization determines macrophage uptake, cytotoxicity, and bioactivity of curcumin nanocrystals. *Int J Pharm*. 2022;626:122133. doi:10.1016/j.ijpharm.2022.122133
19. Gao L, Zhang DR, Chen MH. Drug nanocrystals for the formulation of poorly soluble drugs and its application as a potential drug delivery system. *J Nanopart Res*. 2008;10(5):845–862. doi:10.1007/s11051-008-9357-4
20. McGuckin MB, Wang JW, Ghanma R, et al. Nanocrystals as a master key to deliver hydrophobic drugs via multiple administration routes. *J Control Release*. 2022;345:334–353. doi:10.1016/j.jconrel.2022.03.012
21. Junyaprasert VB, Morakul B. Nanocrystals for enhancement of oral bioavailability of poorly water-soluble drugs. *Asian J Pharm Sci*. 2015;10(1):13–23. doi:10.1016/j.ajps.2014.08.005
22. Zong R, Ruan HA, Zhu WZ, et al. Curcumin nanocrystals with tunable surface zeta potential: preparation, characterization and antibacterial study. *J Drug Deliv Sci Technol*. 2022;76:103771. doi:10.1016/j.jddst.2022.103771

23. Fontana F, Figueiredo P, Zhang P, Hirvonen JT, Liu DF, Santos HA. Production of pure drug nanocrystals and nano co-crystals by confinement methods. *Adv Drug Deliv Rev*. 2018;131:3–21. doi:10.1016/j.addr.2018.05.002
24. Rossetti A, Real DA, Barrientos BA, et al. Significant progress in improving Atorvastatin dissolution rate: physicochemical characterization and stability assessment of self-dispersible Atorvastatin/Tween 80® nanocrystals formulated through wet milling and freeze-drying. *Int J Pharm*. 2024;650:123720. doi:10.1016/j.ijpharm.2023.123720
25. Bhaskar R, Patil PH. Nanocrystal suspension of cefixime trihydrate preparation by high-pressure homogenization formulation design using 2^3 factorial design. *Microb Diver Biotechnol Food Sec*. 2017;9(9):64–71. doi:10.22159/ijpps.2017v9i9.19319
26. Ma YQ, Yang Y, Xie J, Xu JN, Yue PF, Yang M. Novel nanocrystal-based solid dispersion with high drug loading, enhanced dissolution, and bioavailability of andrographolide. *Int J Nanomed*. 2018;13:3763–3779. doi:10.2147/ijn.S164228
27. Tang JL, Xu N, Ji HY, Liu HM, Wang ZY, Wu LH. Eudragit nanoparticles containing genistein: formulation, development, and bioavailability assessment. *Int J Nanomed*. 2011;6:2429–2435. doi:10.2147/ijn.S24185
28. Chen C, Wang L, Cao F, et al. Formulation of 20(S)-protopanaxadiol nanocrystals to improve oral bioavailability and brain delivery. *Int J Pharm*. 2016;497(1):239–247. doi:10.1016/j.ijpharm.2015.12.014
29. Tozuka Y, Miyazaki Y, Takeuchi H. A combinational supercritical CO_2 system for nanoparticle preparation of indomethacin. *Int J Pharm*. 2010;386(1–2):243–248. doi:10.1016/j.ijpharm.2009.10.044
30. Wang WP, Hu J, Sui H, Zhao YS, Feng J, Liu C. Glabridin nanosuspension for enhanced skin penetration: formulation optimization, in vitro and in vivo evaluation. *Pharmazie*. 2016;71(5):252–257. doi:10.1691/ph.2016.5152
31. Li Y, Wang Y, Yue PF, et al. A novel high-pressure precipitation tandem homogenization technology for drug nanocrystals production - a case study with ursodeoxycholic acid. *Pharm Dev Technol*. 2014;19(6):662–670. doi:10.3109/10837450.2013.819015
32. Keating AV, Soto J, Tuleu C, Forbes C, Zhao M, Craig DQM. Solid state characterisation and taste masking efficiency evaluation of polymer based extrudates of isoniazid for paediatric administration. *Int J Pharm*. 2018;536(2):536–546. doi:10.1016/j.ijpharm.2017.07.008
33. Thakkar R, Thakkar R, Pillai A, Ashour EA, Repka MA. Systematic screening of pharmaceutical polymers for hot melt extrusion processing: a comprehensive review. *Int J Pharm*. 2020;576. doi:10.1016/j.ijpharm.2019.118989
34. Shah S, Maddineni S, Lu J, Repka MA. Melt extrusion with poorly soluble drugs. *Int J Pharm*. 2013;453:233–252. doi:10.1016/j.ijpharm.2012.11.001
35. Suryawanshi D, Wavhule P, Shinde U, Kamble M, Amin P. Development, optimization and in-vivo evaluation of cyanocobalamin loaded orodispersible films using hot-melt extrusion technology: a quality by design (QbD) approach. *J Drug Deliv Sci Technol*. 2021;63:102559. doi:10.1016/j.jddst.2021.102559
36. Bookwala M, Thipsay P, Ross S, Zhang F, Bandari S, Repka MA. Preparation of a crystalline salt of indomethacin and tromethamine by hot melt extrusion technology. *Eur J Pharm Biopharm*. 2018;131:109–119. doi:10.1016/j.ejpb.2018.08.001
37. Pimparade MB, Morott JT, Park JB, et al. Development of taste masked caffeine citrate formulations utilizing hot melt extrusion technology and in vitro-in vivo evaluations. *Int J Pharm*. 2015;487(1–2):167–176. doi:10.1016/j.ijpharm.2015.04.030
38. Repka MA, Bandari S, Kallakunta VR, et al. Melt extrusion with poorly soluble drugs - an integrated review. *Int J Pharm*. 2018;535(1–2):68–85. doi:10.1016/j.ijpharm.2017.10.056
39. Martinez-Marcos L, Lamprou DA, Mcburney RT, Halbert GW. A novel hot-melt extrusion formulation of albendazole for increasing dissolution properties. *Int J Pharm*. 2016;499:175–185. doi:10.1016/j.ijpharm.2016.01.006
40. Ye XY, Patil H, Feng X, et al. Conjugation of hot-melt extrusion with high-pressure homogenization: a novel method of continuously preparing nanocrystal solid dispersions. *AAPS Pharm Sci Tech*. 2016;17(1):78–88. doi:10.1208/s12249-015-0389-7
41. Khinast J, Baumgartner R, Roblegg E. Nano-extrusion: a one-step process for manufacturing of solid nanoparticle formulations directly from the liquid phase. *AAPS Pharm Sci Tech*. 2013;14(2):601–604. doi:10.1208/s12249-013-9946-0
42. Li M, Ioannidis N, Gogos C, Bilgili E. A comparative assessment of nanocomposites vs. amorphous solid dispersions prepared via nanoextrusion for drug dissolution enhancement. *Eur J Pharm Biopharm*. 2017;119:68–80. doi:10.1016/j.ejpb.2017.06.003
43. Baumgartner R, Eitzlmayr A, Matsko N, Tetyczka C, Khinast J, Roblegg E. Nano-extrusion: a promising tool for continuous manufacturing of solid nano-formulations. *Int J Pharm*. 2014;477:1–11. doi:10.1016/j.ijpharm.2014.10.008
44. Shi H, Huai S, Wei H, et al. Dissolvable hybrid microneedle patch for efficient delivery of curcumin to reduce intraocular inflammation. *Int J Pharm*. 2023;643:123205. doi:10.1016/j.ijpharm.2023.123205
45. Thorat AA, Dalvi SV. Solid-state phase transformations and storage stability of curcumin polymorphs. *Cryst Growth Des*. 2015;15(4):1757–1770. doi:10.1021/cg501814q
46. Hyun JE, Yi H-Y, Hong G-P, Chun J-Y. Digestion stability of curcumin-loaded nanostructured lipid carrier. *Food Sci Technol*. 2022;162:113474. doi:10.1016/j.lwt.2022.113474
47. Wang Y, Wang C, Zhao J, Ding Y, Li L. A cost-effective method to prepare curcumin nanosuspensions with enhanced oral bioavailability. *J Colloid Interface Sci*. 2017;485:91–98. doi:10.1016/j.jcis.2016.09.003
48. Meng F, Trivino A, Prasad D, Chauhan H. Investigation and correlation of drug polymer miscibility and molecular interactions by various approaches for the preparation of amorphous solid dispersions. *Eur J Pharm Sci*. 2015;71:12–24. doi:10.1016/j.ejps.2015.02.003
49. Patel A, Hu Y, Tiwari JK, Velikov KP. Synthesis and characterisation of zein–curcumin colloidal particles. *Soft Matter*. 2010;6(24):6192–6199. doi:10.1039/c0sm00800a
50. Sanphui P, Goud NR, Khandavilli UBR, Bhanoth S, Nangia A. New polymorphs of curcumin. *Chem Commun*. 2011;47(17):5013–5015. doi:10.1039/c1cc10204d
51. Suresh K, Nangia A. Curcumin: pharmaceutical solids as a platform to improve solubility and bioavailability. *CrystEngComm*. 2018;20:3277–3296. doi:10.1039/c8ce00469b
52. Wang YX, Zhang L, Wang P, Xu XL, Zhou GH. pH-shifting encapsulation of curcumin in egg white protein isolate for improved dispersity, antioxidant capacity and thermal stability. *Food Res Int*. 2020;137109366. doi:10.1016/j.foodres.2020.109366
53. Vardhini NM, Punia J, Jat S, et al. Purification and characterization of pure curcumin, desmethoxycurcumin, and bisdemethoxycurcumin from North-East India Lakadong turmeric (Curcuma longa). *J Chromatogr A*. 2023;1708:464358. doi:10.1016/j.chroma.2023.464358
54. Paswan M, Singh Chandel AK, Malek NI, Dholakiya BZ. Preparation of sodium alginate/Cur-PLA hydrogel beads for curcumin encapsulation. *Int J Biol Macromol*. 2024;254:128005. doi:10.1016/j.ijbiomac.2023.128005

55. Yang D, Wang L, Zhang L, et al. Construction, characterization and bioactivity evaluation of curcumin nanocrystals with extremely high solubility and dispersion prepared by ultrasound-assisted method. *Ultrason Sonochem*. 2024;104:106835. doi:10.1016/j.ultsonch.2024.106835
56. Thommes M, Ely DR, Carvajal MT, Pinal R. Improvement of the Dissolution Rate of Poorly Soluble Drugs by Solid Crystal Suspensions. *Mol Pharm*. 2011;8(3):727–735. doi:10.1021/mp1003493
57. Wang XL, Liao ZG, Zhao GW, et al. Curcumin nanocrystals self-stabilized Pickering emulsion freeze-dried powder: development, characterization, and suppression of airway inflammation. *Int J Biol Macromol*. 2023;245:125493. doi:10.1016/j.ijbiomac.2023.125493
58. Onoue S, Takahashi H, Kawabata Y, et al. Formulation design and photochemical studies on nanocrystal solid dispersion of curcumin with improved oral bioavailability. *J Pharm Sci*. 2010;99(4):1871–1881. doi:10.1002/jps.21964
59. Weibang Y, Zhongming J, Yifei J, Jing J, Min H. The pharmacokinetics of curcumin extract and turmeric monomer after administration in rats. *Pharmacol Clin Chin Mater Med*. 2018;34(5):30–33. doi:10.13412/j.cnki.zyyl.2018.05.008
60. Bangphumi K, Kittiviriyakul C, Towiwat P, Rojsitthisak P, Khemawoot P. Pharmacokinetics of curcumin diethyl disuccinate, a prodrug of curcumin, in Wistar rats. *Eur J Drug Metab Pharmacokinet*. 2016;41:777–785. doi:10.1007/s13318-015-0308-z
61. Xiong W, Sang W, Linghu KG, et al. Dual-functional Brij-S20-modified nanocrystal formulation enhances the intestinal transport and oral bioavailability of berberine. *Int J Nanomed*. 2018;13:3781–3793. doi:10.2147/ijn.S163763
62. Ali HSM, Hanafy AF, Alqurshi A. Engineering of solidified glyburide nanocrystals for tablet formulation via loading of carriers: downstream processing, characterization, and bioavailability. *Int J Nanomed*. 2019;14:1893–1906. doi:10.2147/ijn.S194734
63. Feng Z, Li M, Wang W. Improvement of dissolution and tabletability of carbamazepine solid dispersions with high drug loading prepared by hot-melt extrusion. *Die Pharmazie*. 2019;74(9):523–528. doi:10.1691/ph.2019.9008
64. Wang W, Ye M, Dai A, Feng Z, Li M, Liu Q. Nano-extrusion: a novel and green preparation method for piroxicam nanocrystals. *Basic Clin Physiol Pharmacol*. 2020;127(S1):46–47.
65. Zhang Y-Q. *Application of Hot Melt Extrusion in Preparation of Drug Nanocrystals* [Master of Medicine]. Zhejiang University of Technology; 2022.
66. Xu Y, Zhang X, Di L, Fan W. Preparation of thermosensitive curcumin solid dispersions by hot-melt extrusion technique. *Chin Trad Herbal Drugs*. 2018;49(17):4014–4021. doi:10.7501/j.issn.0253-2670.2018.17.008
67. Yarlagadda DL, Anand VSK, Nair AR, et al. A computational-based approach to fabricate Ceritinib co-amorphous system using a novel co-former Rutin for bioavailability enhancement. *Eur J Pharm Biopharm*. 2023;190:220–230. doi:10.1016/j.ejpb.2023.07.019
68. Li J, Wang X, Yu D, Zhoujin Y, Wang K. Molecular complexes of drug combinations: a review of cocrystals, salts, coamorphous systems and amorphous solid dispersions. *Int J Pharm*. 2023;648:123555. doi:10.1016/j.ijpharm.2023.123555
69. Xu X, Grohganz H, Rades T. Influence of Water on Amorphous Lidocaine. *Mol Pharm*. 2022;19:3199–3205. doi:10.1021/acs.molpharmaceut.2c00339
70. Simões MF, Pinto RMA, Simões S. Hot-melt extrusion: a roadmap for product development. *AAPS Pharm Sci Tech*. 2021;22(5):184. doi:10.1208/s12249-021-02017-7